Applied Chemical Engineering (2025) Volume 8 Issue 2 ISSN: 2578-2010 (O)
doi: 10.59429/ace.v8i2.5704

RESEARCH ARTICLE

Development of bioactive heterocyclic compounds from trimethoprim: A new approach toward anticancer agents

Rana Hussein Alwan[1], May Jaleel Abed[1*]

[1*] *Department of Chemistry, College of Education, University of Al-Qadisiyah, Diwaniyah, 54004, Iraq*

***Corresponding author:** May Jaleel Abed; may.abed@qu.edu.iq

ABSTRACT

This study presents the synthesis and characterization of novel heterocyclic derivatives derived from trimethoprim through diazotization, aldol condensation, and cyclization reactions. Azo (A1), chalcone (A2, A6), pyrazoline (A3, A7), thiazine (A4, A8), and oxazine (A5, A9) derivatives were successfully prepared and structurally confirmed using FT-IR, ^{1}H-NMR, and ^{13}C-NMR spectroscopy. The synthesized compounds displayed diverse physical properties, indicating structural complexity and variation in polarity and thermal stability. Their biological evaluation against colon cancer (HRT) cells revealed significant cytotoxic activity. Thiazine derivative (A8) exhibited an IC_{50} value of 206.7 µg/mL. The oxazine derivative (A9) demonstrated superior activity with an IC_{50} of 0.1669 µg/mL (0.231 µmol/L), compared to the reference drug 5-fluorouracil (IC_{50} = 3.73 µmol/L). These results highlight the potential of trimethoprim-derived heterocyclic scaffolds as anticancer agents. The study contributes to ongoing efforts in medicinal chemistry to develop effective therapeutic compounds by modifying existing antibiotic structures to enhance biological activity and target specificity in cancer treatment.

Keywords: Trimethoprim derivatives; Chalcone derivative; Pyrazoline derivative; Anticancer activity and Cyclization reaction

ARTICLE INFO

Received: 15 May 2025
Accepted: 4 June 2025
Available online: 30 June 2025

1. Introduction

The development of novel heterocyclic compounds has emerged as a cornerstone of modern pharmaceutical research, driven by the urgent need for new therapeutic agents to combat evolving microbial resistance and address unmet medical needs. Among the diverse array of heterocyclic scaffolds, nitrogen and sulfur-containing compounds have garnered significant attention due to their remarkable biological activities and structural versatility [1-3]. The synthesis and characterization of pyrazoline, oxazine, and thiazine derivatives represent a particularly promising avenue in medicinal chemistry, offering potential solutions to contemporary healthcare challenges. Trimethoprim, a well-established antibiotic primarily utilized for the treatment of urinary tract infections, serves as an excellent starting material for the development of novel heterocyclic compounds [4]. This synthetic antibiotic functions by inhibiting bacterial dihydrofolate reductase and has demonstrated remarkable efficacy against a broad spectrum of gram-positive and gram-negative bacteria [5]. The unique structural features of trimethoprim, including its pyrimidine core and methoxy-substituted benzyl moiety, provide an ideal foundation for chemical modifications that can lead to the discovery of new bioactive molecules. Pyrazoline derivatives, characterized by their five-

membered ring structure containing two nitrogen atoms, have demonstrated exceptional biological activities including anticancer, antimicrobial, anti-inflammatory, and antioxidant properties [6, 7]. These electron-rich nitrogenous heterocycles have attracted considerable attention from medicinal chemists due to their structural stability and diverse pharmacological profiles. Recent studies have highlighted the potential of pyrazoline compounds as therapeutic targets for various diseases, with particular emphasis on their role as nitric oxide synthase inhibitors and cannabinoid CB1 receptor antagonists [8-11]. Oxazine compounds, featuring a six-membered ring containing one oxygen and one nitrogen atom, have emerged as promising scaffolds in pharmaceutical research. These heterocyclic systems exhibit a wide variety of biological activities, including anticancer, antimicrobial, anti-inflammatory, and antiplatelet properties [12-16].

The versatility of oxazine derivatives in medicinal chemistry is further enhanced by their ability to serve as intermediates in the synthesis of more complex bioactive molecules [17]. Thiazine derivatives, containing both sulfur and nitrogen atoms within their heterocyclic framework, represent another class of compounds with significant pharmaceutical potential. These molecules have demonstrated remarkable biological activities, including antibacterial, antifungal, antitumor, and antimalarial properties [18-22]. The presence of sulfur and nitrogen elements in thiazine compounds contributes to their excellent biological activity, with the position of these heteroatoms playing a crucial role in determining their pharmacological properties [23]. The synthesis of these heterocyclic compounds often involves the use of chalcone derivatives as key intermediates. Chalcones, characterized by their α, β-unsaturated carbonyl system, serve as versatile building blocks in organic synthesis and have been extensively utilized in the preparation of various heterocyclic compounds [24, 25]. These compounds not only function as important synthetic intermediates but also possess significant biological activities, including antibacterial, antifungal, anti-inflammatory, and anticancer properties.

The current research focuses on the synthesis and characterization of new pyrazoline, oxazine, and thiazine compounds derived from trimethoprim through a series of well-designed chemical transformations. This investigation aims to explore the potential of these novel heterocyclic derivatives as promising candidates for pharmaceutical applications, with particular emphasis on their antimicrobial and anticancer activities. The systematic approach employed involves the initial preparation of azo and chalcone derivatives from trimethoprim, followed by their subsequent conversion to the target heterocyclic compounds through cyclization reactions. The significance of this research extends beyond the mere synthesis of new compounds, as it contributes to the growing body of knowledge regarding structure-activity relationships in heterocyclic chemistry. By systematically modifying the trimethoprim scaffold and introducing various heterocyclic moieties, this study provides valuable insights into the factors that influence biological activity and pharmacological properties.

2. Chemicals and reagents

All chemicals and reagents used in this study were of analytical grade and used without further purification. Trimethoprim (TMP), 4-hydroxyacetophenone, furfuryl aldehyde, 4-bromobenzaldehyde, 2,4-dinitrophenylhydrazine, thiourea, urea, sodium nitrite, sodium hydroxide (NaOH), hydrochloric acid (HCl), and glacial acetic acid were purchased from Sigma-Aldrich and Merck. Absolute ethanol and distilled water were used throughout all synthetic procedures. Thin-layer chromatography (TLC) was performed using pre-coated silica gel plates and a solvent system of benzene:methanol (4:1) for monitoring reaction progress.

2.1. Synthesis of azo derivative (A1)

A solution of trimethoprim (TMP) (0.01 mol, 0.29 g) was prepared in 30 mL of distilled water containing concentrated hydrochloric acid (4N). The mixture was cooled to 0 °C, and a freshly prepared solution of sodium nitrite (0.01 mol in 30 mL) was added dropwise with continuous stirring. The diazotization reaction was maintained at 0 °C for 20 minutes to ensure complete conversion to the diazonium salt. The resulting

diazonium solution was then added slowly to a mixture of 4-hydroxyacetophenone (0.01 mol) dissolved in 10 mL ethanol and 30 mL of 5% sodium hydroxide solution. The mixture was stirred for 1 hour at room temperature, during which a brown precipitate formed. The product was filtered, washed with distilled water several times, dried, and recrystallized from ethanol (**Figure 1).**

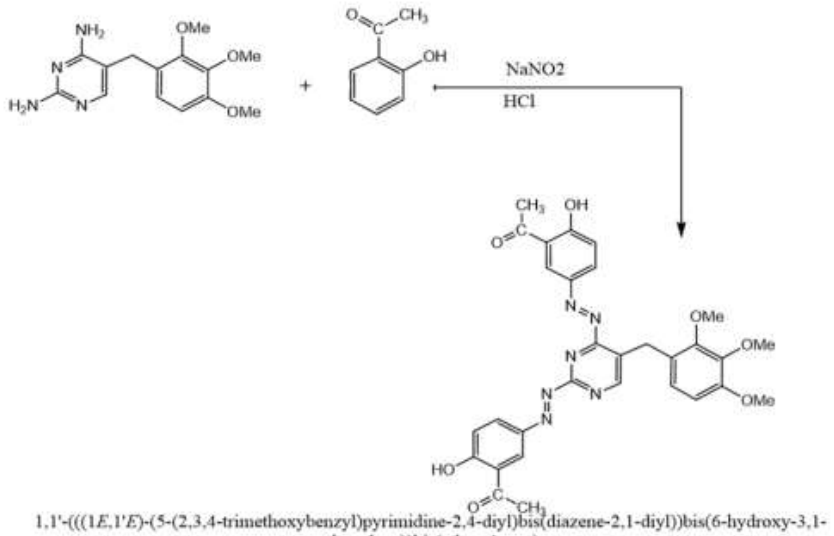

Figure 1. Proposed synthetic pathway for the preparation of azo-linked trimethoprim derivative via diazotization–coupling reaction

2.2. Synthesis of chalcone derivative (A2)

A solution of the azo compound A1 (0.0017 mol, 1.00 g) was dissolved in 25 mL of absolute ethanol with stirring until fully dissolved. Furfuryl aldehyde (0.001 mol, 0.33 mL) was then added, followed by dropwise addition of 10 mL of 10% sodium hydroxide. The reaction mixture was stirred at room temperature (25 °C) for 12–20 hours. After reaction completion (monitored by TLC using benzene:methanol = 4:1), the mixture was acidified with 2N HCl. The resulting product was filtered and recrystallized from ethanol (**Figure 2**).

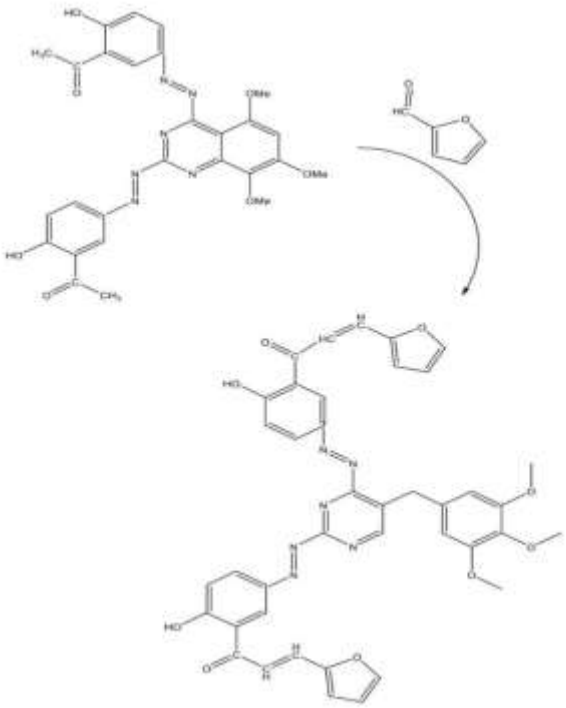

Figure 2. Synthetic route for azo–chalcone hybrid derivatives

2.3. Synthesis of pyrazoline derivative (A3)

The chalcone A2 (0.001 mol, 0.74 g) was dissolved in 35 mL of absolute ethanol under stirring. 2,4-Dinitrophenylhydrazine (0.002 mol, 0.4 g) and a few drops of glacial acetic acid were added. The reaction mixture was refluxed for 23–27 hours, and its progress was monitored by TLC (benzene: methanol = 4:1). Upon completion, the mixture was cooled, filtered, and the solid product was washed and recrystallized from ethanol (**Figure 3**).

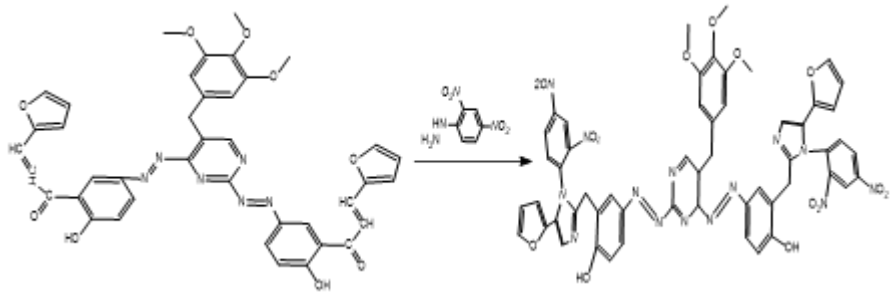

Figure 3. Proposed synthetic pathway for the preparation of pyrazoline derivative via cyclization of chalcone intermediate using 2× 2,4-dinitrophenylhydrazine

2.4. Synthesis of thiazine derivative (A4)

Chalcone A2 (0.001 mol, 0.74 g) was dissolved in 10 mL of alcoholic sodium hydroxide. Thiourea (0.002 mol) was added to the solution, and the reaction mixture was refluxed for 24–32 hours. The reaction was monitored by TLC. After completion, the mixture was poured into cold water, and the precipitate was filtered, washed, dried, and recrystallized from ethanol (**Figure 4**).

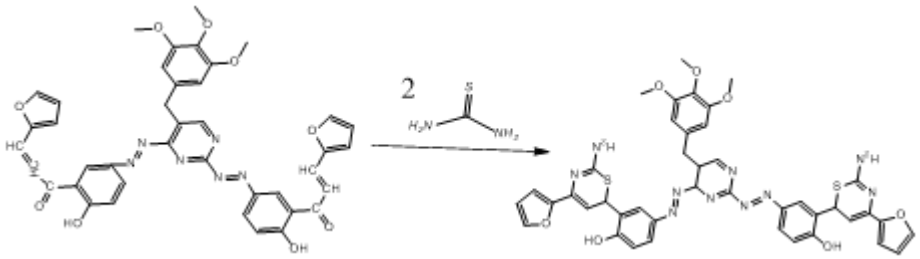

Figure 4. Proposed synthetic pathway for the preparation of thiazine derivative via condensation of chalcone intermediate with thiourea under alkaline conditions

2.5. Synthesis of oxazine derivative (A5)

Chalcone A2 (0.001 mol, 0.74 g) was dissolved in 10 mL of alcoholic sodium hydroxide. Urea (0.002 mol) was added, and the mixture was refluxed for 24–32 hours. TLC (benzene: methanol = 4:1) was used to monitor the progress. After cooling, the mixture was poured into cold water, and the precipitate was collected, washed, and recrystallized from ethanol (**Figure 5**).

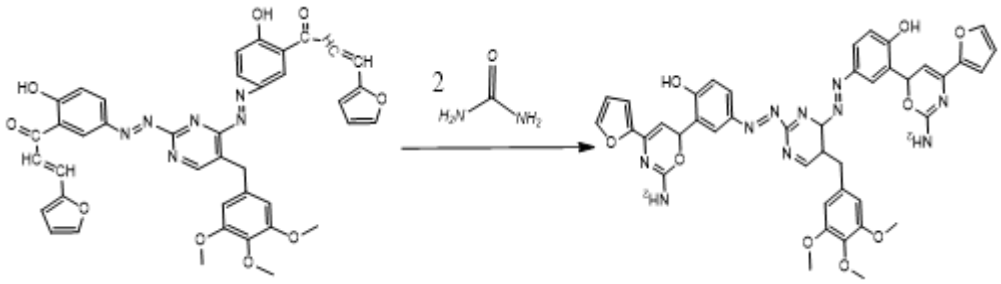

Figure 5. Proposed synthetic pathway for the preparation of oxazine derivative via condensation of chalcone intermediate with urea under alkaline conditions

2.6. Synthesis of chalcone derivative (A6)

The azo compound A1 (0.0017 mol, 1.00 g) was dissolved in 25 mL of absolute ethanol. To this solution, 4-bromobenzaldehyde (0.002 mol, 0.634 g) was added, followed by dropwise addition of 10 mL of 10% sodium hydroxide. The mixture was stirred for 12–20 hours at room temperature. After acidification with 0.2N HCl, the mixture was filtered and the product recrystallized from ethanol. TLC was used to confirm the reaction completion (**Figure 6**).

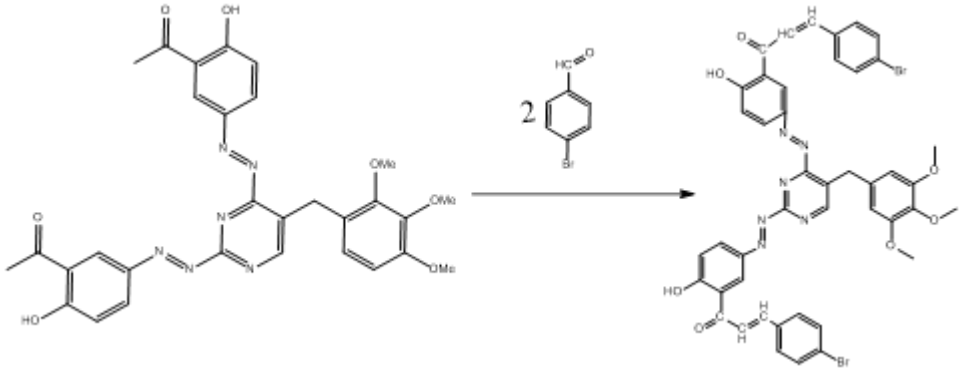

Figure 6. Proposed synthetic pathway for the preparation of bromo-substituted chalcone derivative via Claisen–Schmidt condensation of azo-linked trimethoprim with 4-bromobenzaldehyde

2.7. Synthesis of pyrazoline derivative (A7)

The chalcone A6 (0.001 mol, 0.92 g) was dissolved in 35 mL of absolute ethanol. To this, 2,4-dinitrophenylhydrazine (0.4 g) and 5 drops of glacial acetic acid were added. The mixture was refluxed for 23–27 hours and monitored via TLC. The final product was obtained by filtration, washing, and recrystallization from ethanol (**Figure 7**).

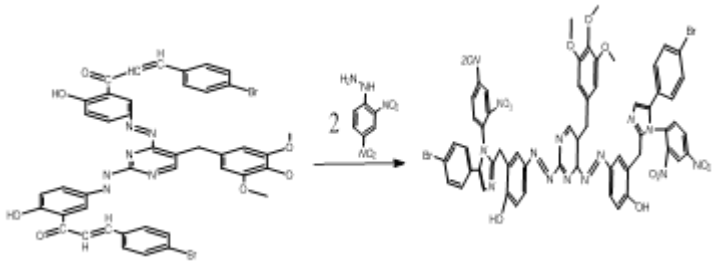

Figure 7. Proposed synthetic pathway for the preparation of pyrazoline derivative via cyclization of bromo-chalcone intermediate using 2,4-dinitrophenylhydrazine

2.8. Synthesis of thiazine derivative (A8)

Chalcone A6 (0.001 mol, 0.918 g) was dissolved in 10 mL of alcoholic sodium hydroxide. Thiourea (0.002 mol) was added, and the mixture was refluxed for 24–32 hours. TLC confirmed reaction progress. The product was precipitated in cold water, filtered, washed, and recrystallized from ethanol (**Figure 8**).

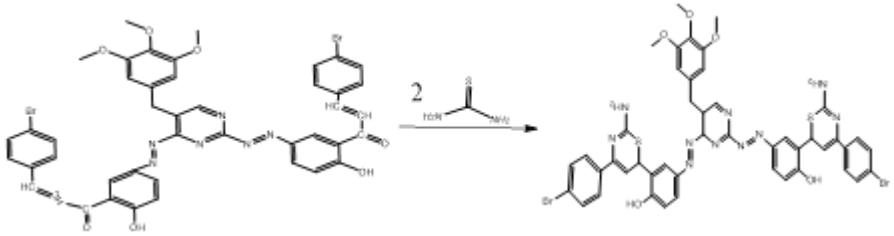

Figure 8. Proposed synthetic pathway for the preparation of thiazine derivative via condensation of bromo-chalcone intermediate with thiourea under alkaline conditions

2.9. Synthesis of oxazine derivative (A9)

Chalcone A6 (0.001 mol, 0.82 g) was dissolved in 10 mL of alcoholic sodium hydroxide. Urea (0.002 mol) was added, and the mixture was refluxed for 24–32 hours. After confirming reaction completion by TLC, the mixture was cooled, poured into cold water, and the precipitate was filtered, washed, and recrystallized from ethanol (**Figure 9**).

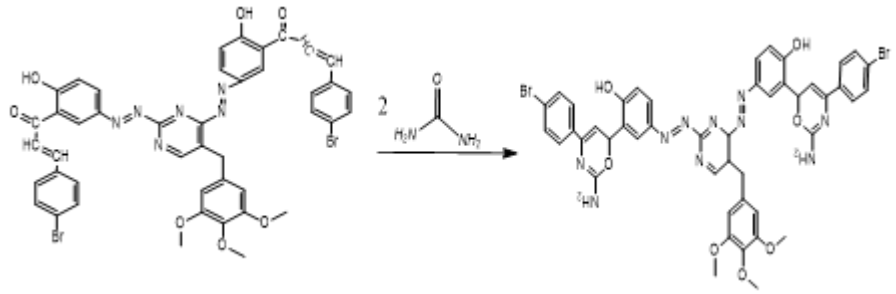

Figure 9. Proposed synthetic pathway for preparation of oxazine derivative via condensation of bromo-chalcone intermediate with urea under alkaline conditions

3. Discussion of physical properties of synthesized trimethoprim-based derivatives

The physical characteristics of the synthesized heterocyclic compounds derived from trimethoprim are systematically presented in **Table 1.**

Table 1. Physical Properties of Synthesized Compounds

No.	Molecular Formula (M.F)	Molecular Weight (g/mol)	Melting Point (°C)	Color	R_f (Benzene: Methanol 1:4)	Yield (%)
1	$C_{30}H_{28}N_6O_7$	584.25	240–245	Dark Yellow	0.42	80–85
2	$C_{40}H_{32}N_6O_9$	740.28	250–255	Orange-Red	0.35	75–80
3	$C_{54}H_{42}N_{14}O_{15}$	1127.01	315–325	Light Red	0.25	70–75
4	$C_{42}H_{38}N_{10}O_7S_2$	858.95	230–235	Orange	0.45	78–83
5	$C_{42}H_{38}N_{10}O_9$	826.28	235–240	Orange-Red	0.35	75–80
6	$C_{44}H_{34}Br_2N_6O_7$	918.6	245–255	Brown to Dark Brown	0.3	65–70
7	$C_{58}H_{44}Br_2N_{14}O_{13}$	1304.88	335–345	Dark Brown	0.22	60–65
8	$C_{46}H_{40}Br_2N_{10}O_5S_2$	1036.82	260–270	Dark Purple	0.28	70–75
9	$C_{46}H_{40}Br_2N_{10}O_7$	1004.14	268–275	Red-Purple	0.32	70–75

This set includes various derivatives such as azo, chalcone, pyrazoline, thiazine, and oxazine, each exhibiting distinctive physicochemical features that reflect their structural diversity and functional complexity. The molecular formulas (M.F) and corresponding molecular weights (M.Wt) illustrate the progressive increase in structural complexity across the compounds. For example, compound A1, a relatively simpler azo derivative, has a molecular weight of 584.25 g/mol, whereas compound A7, a heavily substituted pyrazoline derivative, reaches 1304.88 g/mol, highlighting the incorporation of bulky functional groups like nitrophenyl and bromophenyl moieties. The melting points of the compounds, ranging from 230 °C to 345 °C, provide insight into their thermal stability. Higher melting points, as observed in A7 (335–345 °C) and A9 (268–275 °C), are indicative of strong intermolecular interactions, extended conjugation, and overall molecular rigidity. These characteristics are commonly associated with compounds containing multiple aromatic rings and hydrogen-bonding donors or acceptors. The colors of the compounds range from dark yellow to reddish-purple, consistent with presence of extended π-conjugation systems as azo linkages and chalcone frameworks, which

often result in chromophoric behavior and potential optical activity. These visible colorations may also indicate potential applications in dye or pigment chemistry. The R_f values, obtained via Thin Layer Chromatography (TLC) using a benzene:methanol (1:4) mobile phase, ranged between 0.22 and 0.45. These values reflect the polarity of the compounds; lower Rf values suggest higher polarity and stronger interaction with stationary phase. Compounds with hydrophilic substituents (e.g., nitro or hydroxyl groups) tend to migrate slower, which is consistent with observed data.

3.1. Determination of effect of ligands and prepared complexes on HRT cell inhibition by MTT assay

The colon cancer cell line (HRT) was exposed to concentrations of (31.25-1000) µg/mL of either Thiazine Derivative (A8), or Oxazine Derivative (A9), for 24 hours and at a temperature of 37 °C. Toxicity was evaluated based on the percentages of growth inhibition rate compared to the not-treated colon cancer cell.

3.2. Discussion

The synthesized heterocyclic derivatives of trimethoprim were characterized using spectroscopic techniques including FT-IR (identifying its functional groups and molecular structure based on how it absorbs infrared light [26-30], ^{1}H-NMR, and ^{13}C-NMR (to confirm the successful formation of azo, chalcone, pyrazoline, thiazinez, and oxazine derivatives through a series of diazotization, aldol condensation, and cyclization reactions). Each compound exhibited unique spectral features consistent with its proposed structure.

3.3. Azo derivative (A1)

The FT-IR spectrum (**Figure 10a**) of A1 displayed a broad absorption at 3400–3300 cm^{-1} corresponding to phenolic O–H stretching, while a sharp band at 1695–1665 cm^{-1} indicated the carbonyl (C=O) stretch of the aromatic ketone [19, 20]. The azo linkage (N=N) was evident in the 1600–1450 cm^{-1} range. The ^{1}H-NMR spectrum (**Figure 10b**) confirmed the presence of methoxy (δ ≈ 3.74 ppm), aromatic (δ 7.96–7.49 ppm), and phenolic (δ 11.00 ppm) protons. The ^{13}C-NMR (**Figure 10c**) showed downfield shifts at δ ~198–204 ppm due to C=O carbons, and signals between 106–166 ppm confirmed the aromatic backbone [31,40].

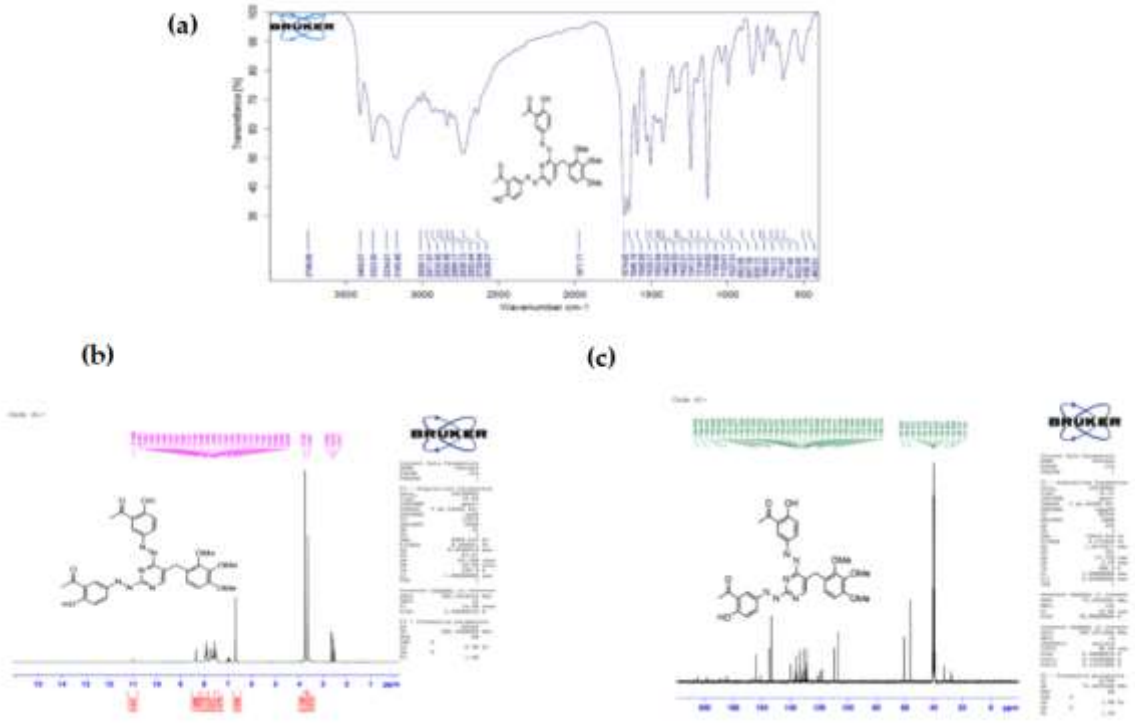

Figure 10. (a) FTIR, (b) ^{1}H-NMR spectrum and (c) ^{13}C-NMR spectrum of azo derivative (A1)

3.4. Chalcone derivative (A2)

The FT-IR spectrum (**Figure 11a**) showed key features of hydroxyl (3400–3200 cm^{-1}), aliphatic and aromatic C–H (3100–2800 cm^{-1}), and a strong ketonic C=O band near 1690 cm^{-1} [16,21,22]. Aromatic C=C and azo vibrations were also observed. The ^{1}H-NMR spectrum (**Figure 11b**) showed vinylic protons at δ 8.27 and 8.03 ppm, confirming the α, β-unsaturated ketone moiety, along with phenolic and methoxy groups. The ^{13}C-NMR (**Figure 11c**) supported this, with C=O carbons appearing around δ ~180–189 ppm [32].

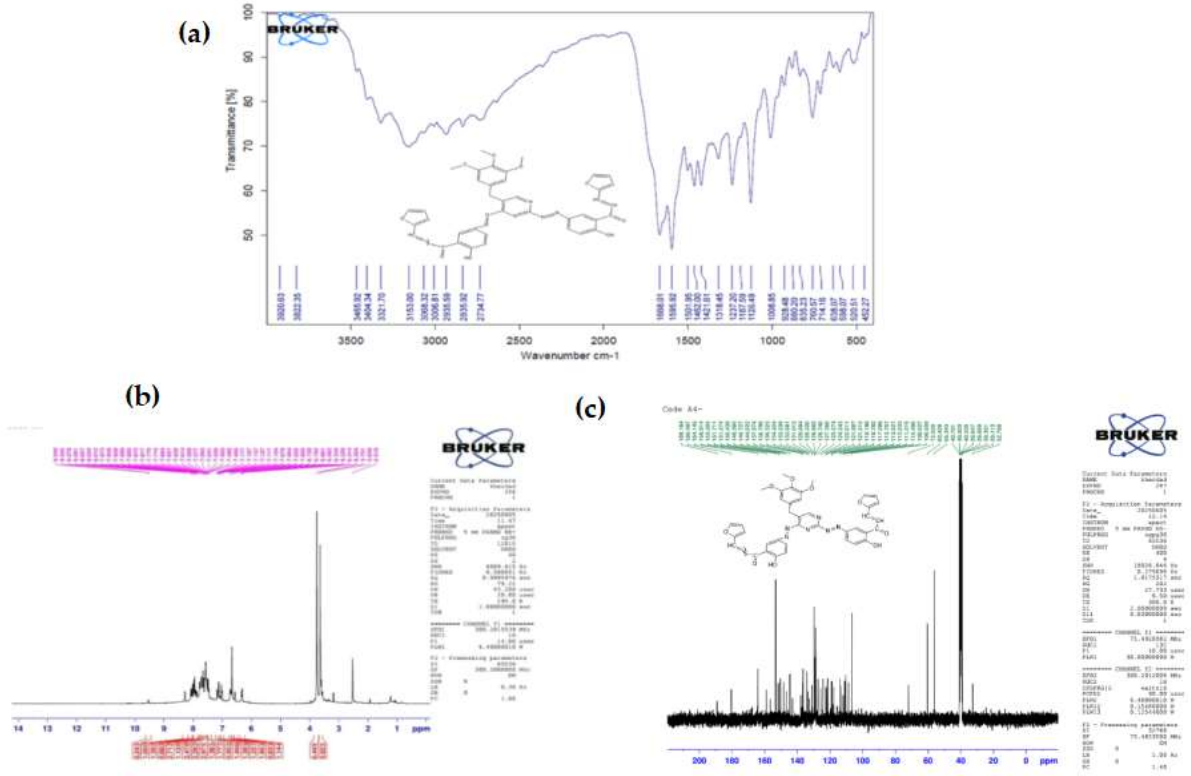

Figure 11. (a) FTIR, (b) ^{1}H-NMR spectrum and (c) ^{13}C-NMR spectrum of Chalcone Derivative (A2)

3.5. Pyrazoline Derivative (A3)

FT-IR analysis (**Figure 12a**) of A3 revealed phenolic O–H (3408–3368 cm^{-1}), aliphatic C–H (2922–2857 cm^{-1}), and C=N stretching (1682 cm^{-1}), indicating ring closure. The presence of diazenyl or unsaturated nitrogen was suspected from peaks around 2121 and 2050 cm^{-1}. The ^{1}H-NMR spectrum (**Figure 12b**) confirmed pyrazoline ring formation with methylene protons (δ 5.64 ppm) and maintained aromatic and methoxy environments [33].

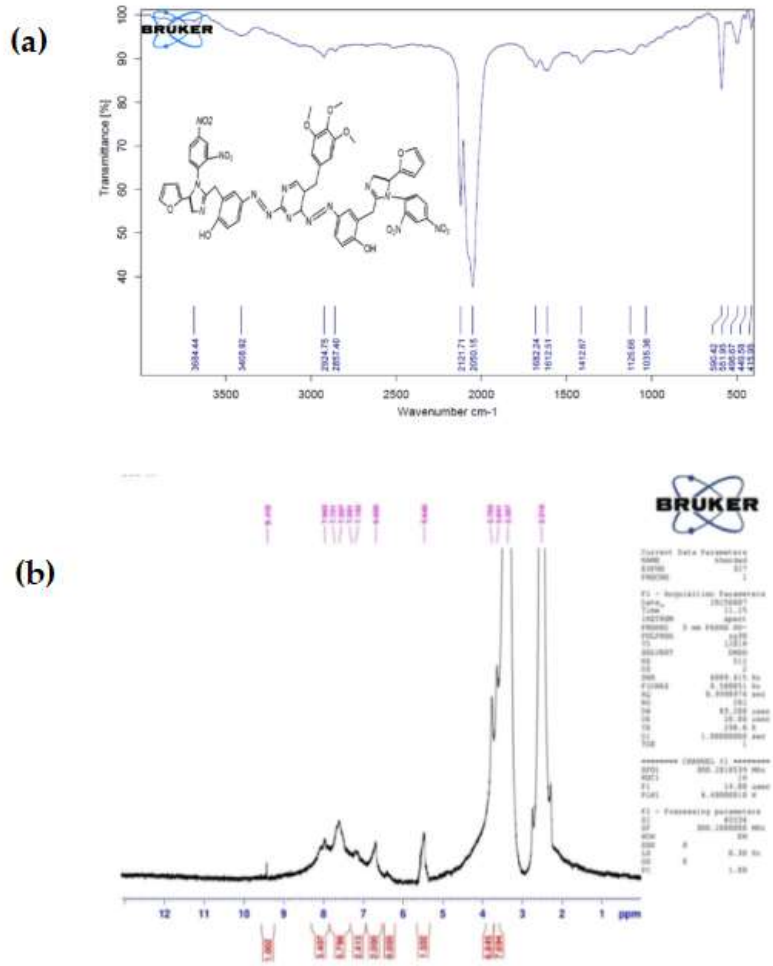

Figure 12. (a) FTIR and (b) ^{1}H-NMR spectrum of Pyrazoline Derivative (A3)

3.6. Thiazine Derivative (A4)

The FT-IR spectrum (**Figure 13a**) showed O–H stretching at 3382–3170 cm^{-1}, C=O at 1690 cm^{-1}, and additional bands for aromatic, azo, and C–N vibrations. In ^{1}H-NMR (**Figure 13b**), distinctive signals were seen for methylene (δ 5.71 ppm), amino (δ 6.55 ppm), and phenolic protons (δ 9.42 ppm). The ^{13}C-NMR (**Figure 13c**) data supported the presence of aromatic, methoxy, and thiazine-related carbon environments [34].

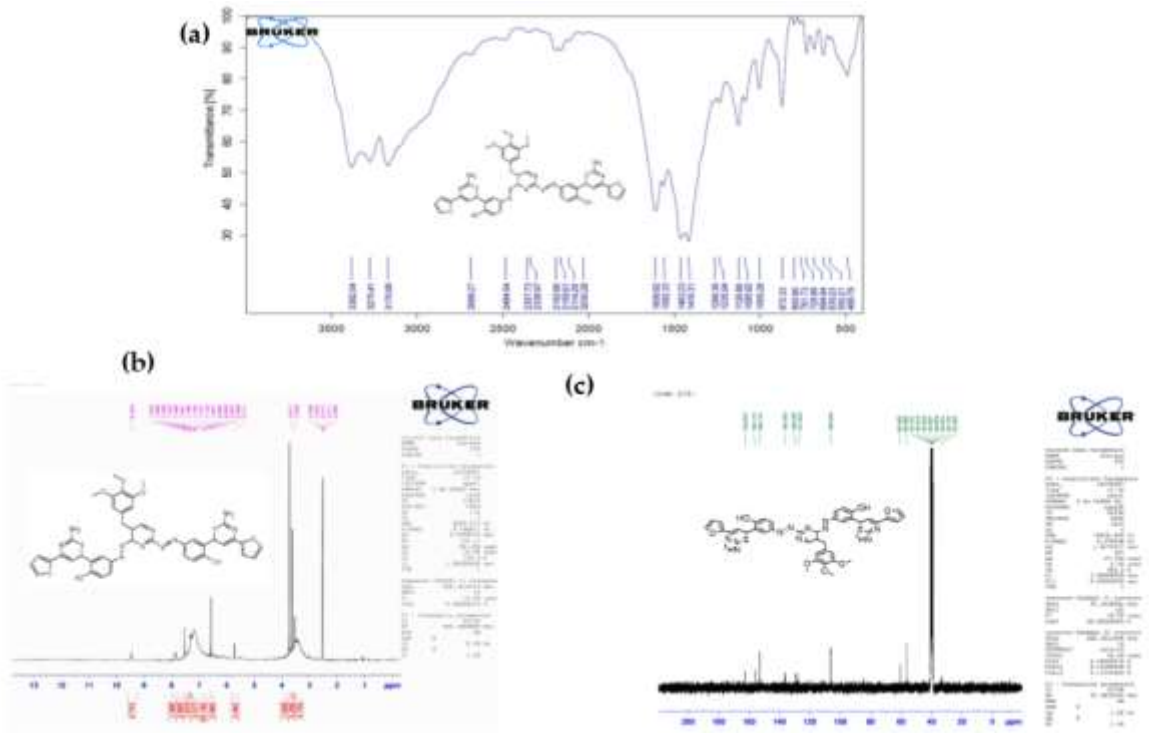

Figure 13. (a) FTIR, (b) ^{1}H-NMR spectrum and (c) ^{13}C-NMR spectrum of Thiazine Derivative (A4)

3.7. Oxazine derivative (A5)

The FT-IR spectrum (**Figure 14a**) of A5 showed O–H and N–H stretching (3445–3349 cm^{-1}), strong C=N/C=C absorptions (1613–1586 cm^{-1}), and methoxy-related C–O bands (1220–1030 cm^{-1}). The ^{1}H-NMR spectrum (**Figure 14b**) displayed typical signals for methylene (δ 5.55 ppm), amino (δ 6.14 ppm), and phenolic protons (δ 9.48 ppm), indicating successful formation of the oxazine ring. The ^{13}C-NMR (**Figure 14c**) data confirmed the presence of aromatic and heterocyclic carbon centers [35].

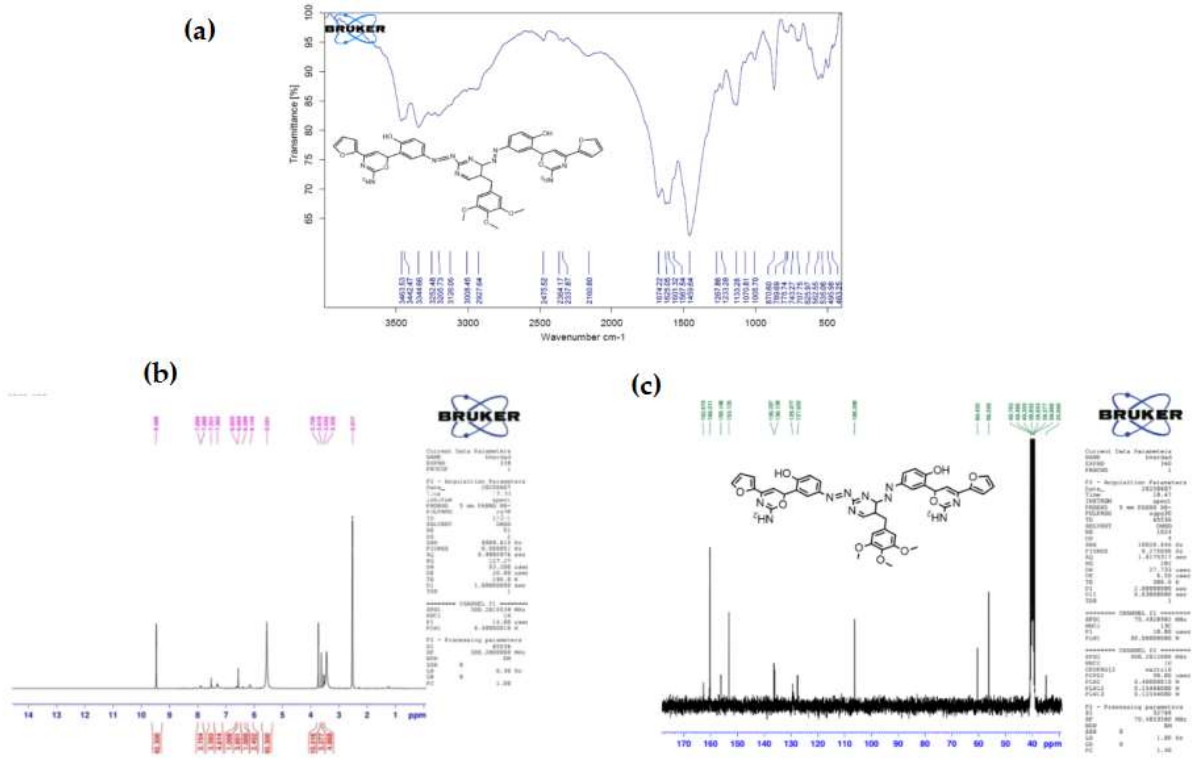

Figure 14. (a) FTIR, (b) ^{1}H-NMR spectrum and (c) ^{13}C-NMR spectrum of Oxazine Derivative (A5)

3.8. Second chalcone derivative (A6)

FT-IR bands (**Figure 15a**) at 3400–3200 cm^{-1} and 1590 cm^{-1} confirmed phenolic O–H and C=N of pyridine rings. The ^{1}H-NMR spectrum (**Figure 15b**) exhibited vinylic protons (δ ~8.31 ppm) and aromatic/methoxy signals. The presence of C–Br was confirmed by FT-IR bands at 850–650 cm^{-1} and corroborated by downfield ^{13}C shifts (**Figure 15c**) around 190–197 ppm for the C=O group [36].

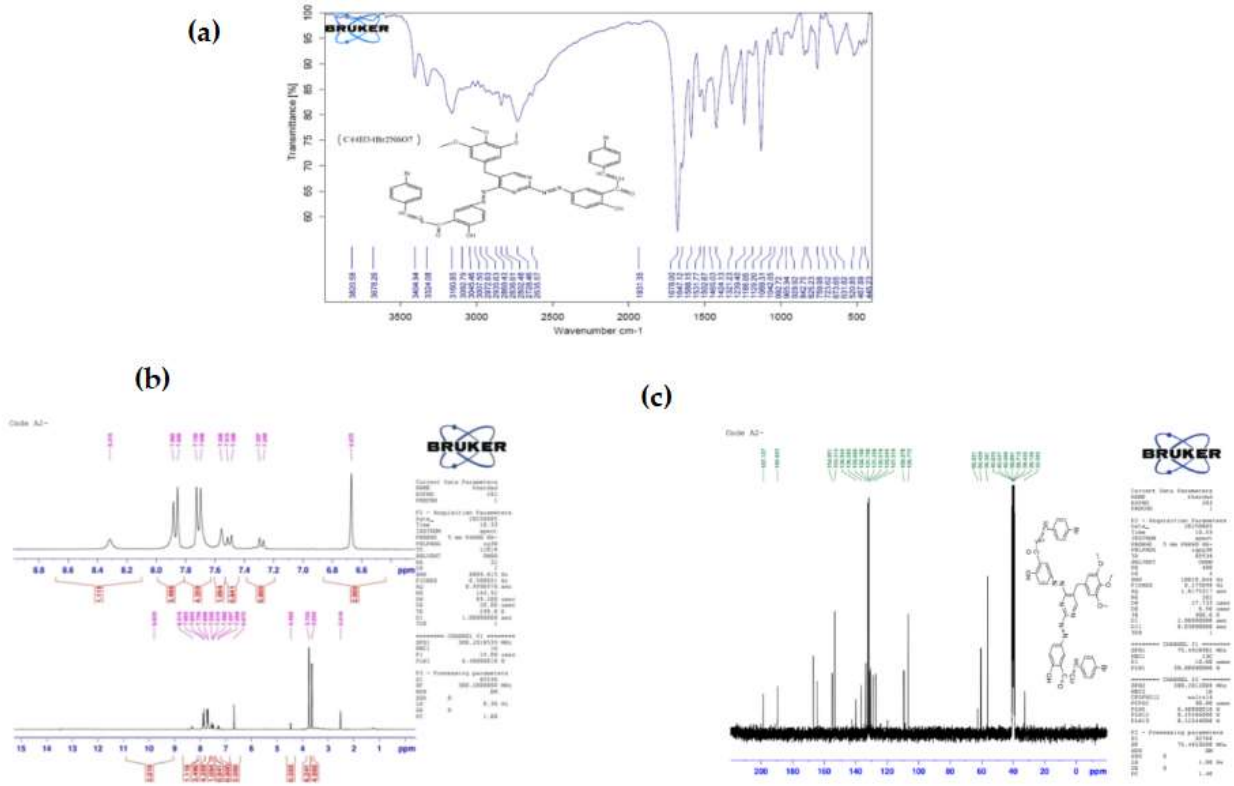

Figure 15. (a) FTIR, (b) ^{1}H-NMR spectrum and (c) ^{13}C-NMR spectrum of Chalcone Derivative (A6)

3.9. Pyrazoline derivative (A7)

This compound exhibited a complex FT-IR pattern (**Figure 16a**) with bands for O–H, C=O, nitro, and methoxy groups. The ^{1}H-NMR spectrum (**Figure 16b**) showed crowded aromatic environments (23H), methylene (δ 5.68 ppm), and methoxy (15H) [36].

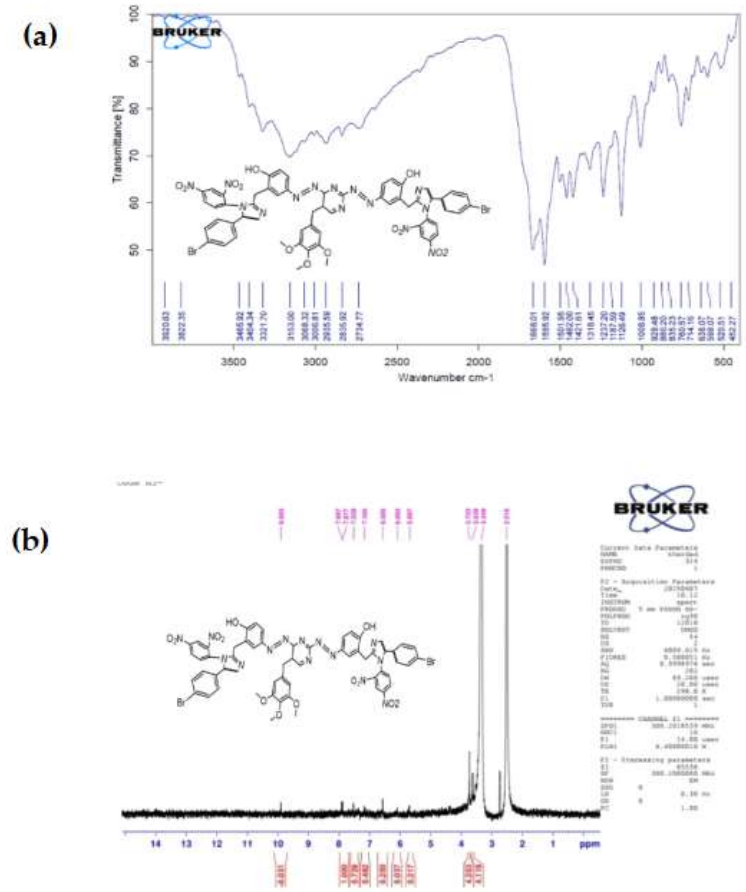

Figure 16. (a) FTIR and (b) ^{1}H-NMR spectrum of Pyrazoline Derivative (A7)

3.10. Thiazine derivative (A8)

FT-IR spectra (**Figure 17a**) confirmed C=N (1650–1600 cm^{-1}), C–N, and C–O functionalities, with additional support for C–Br bonds. ^{1}H-NMR (**Figure 17b**) revealed amino (δ 6.11 ppm), methylene (δ 5.71 ppm), and aromatic protons. ^{13}C-NMR (**Figure 17c**) resonances at 106–164 ppm supported a highly substituted aromatic and thiazine-containing system [37].

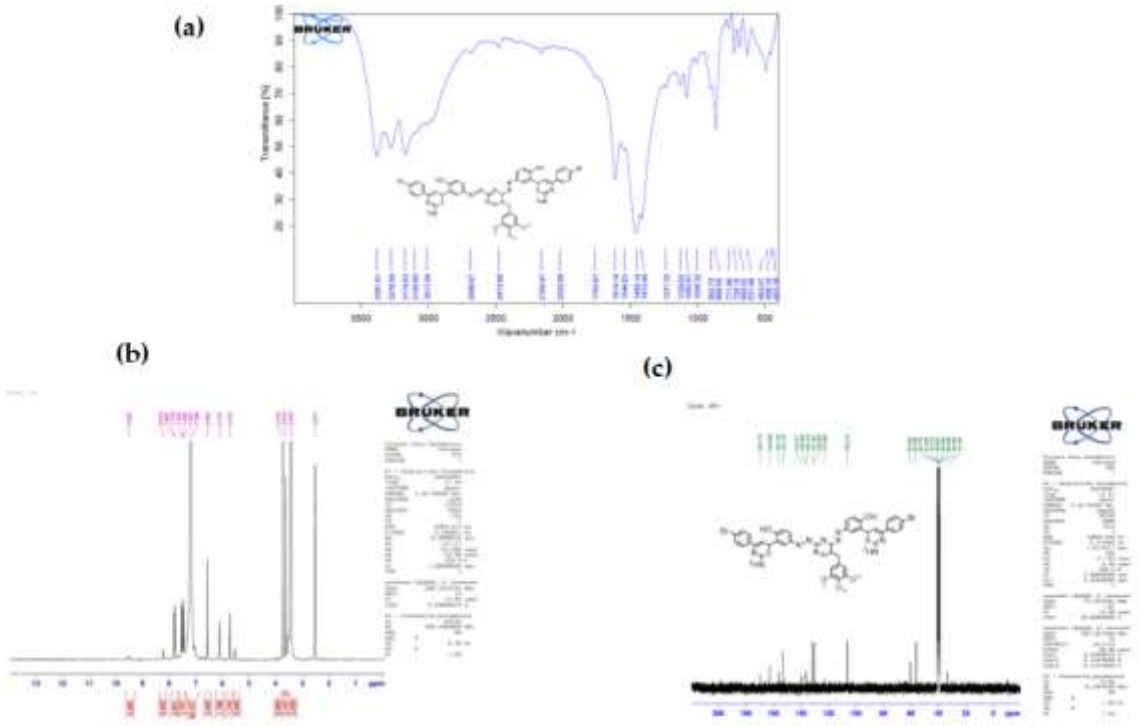

Figure 17. (a) FTIR, (b) ^{1}H-NMR spectrum and (c) ^{13}C-NMR spectrum of Thiazine Derivative (A8)

3.11. Oxazine derivative (A9)

FT-IR (**Figure 18a**) showed O–H, C–H, and C=O stretches, along with azo, methoxy, and aromatic fingerprints. The ^{1}H-NMR spectrum (**Figure 18b**) revealed phenolic (δ 9.69 ppm), amino (δ 6.55 ppm), and methylene protons (δ 5.50 ppm). The ^{13}C-NMR (**Figure 18c**) data showed aromatic carbons and methylene groups consistent with the oxazine structure [37].

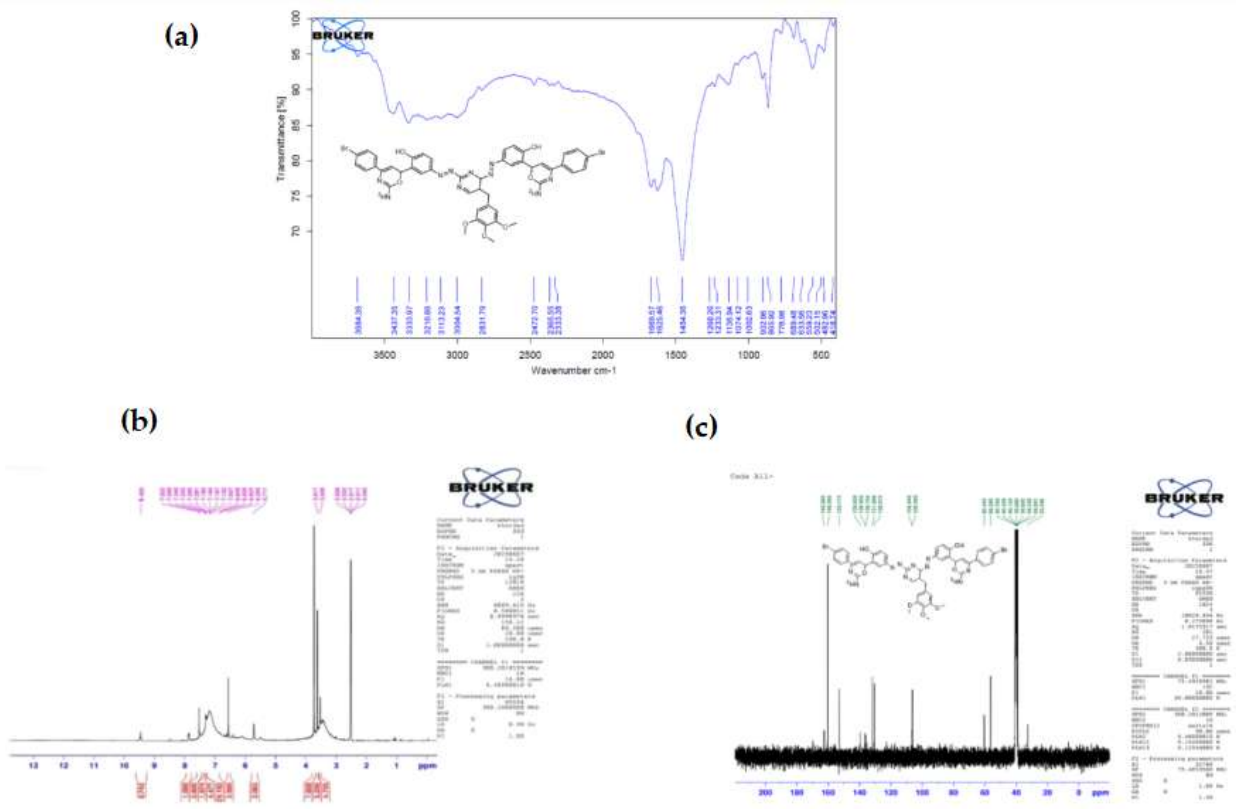

Figure 18. (a) FTIR, (b) ^{1}H-NMR spectrum and (c) ^{13}C-NMR spectrum of Oxazine Derivative (A9)

3.12. Investigation of effect of Thiazine Derivative (A8) on growth of colon cancer cell lines (HRT)

The results in **Figure 19** and **Table 2** showed that the lowest percentage of inhibition for colon cancer cell lines at a concentration of 31.25 (µg/ml), and the highest percentage of inhibition was at a concentration of 250 (µg / ml), where the inhibition percentage of Derivative (A8) of the colon cancer cell line at the concentration 250(µg/ml) was (73.60%), which is an excellent result, and this in turn indicates the possibility of using this complex as a treatment for colon cancer. The half-inhibition concentration fifty (IC_{50}) of Derivative (A8) with the colon cancer cell line (HRT) was 206.7 (µg / ml) [38].

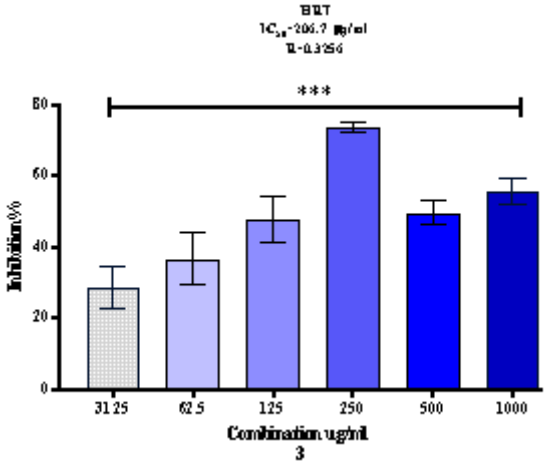

Figure 19. Comparison of mean values of Derivative (A8) in different concentrations. The Figure shows a significant difference among concentrations (p-value<0.0001). Data are expressed as means ± SEM

Table 2. Comparison of mean values of Derivative (A8) in different concentrations

Concentration µg/ml	31.25	62.5	125	250	500	1000
Number of values	4	4	4	4	4	4
Minimum	19.65	16.62	31.75	69.07	40.83	50.92
Maximum	45.54	48.23	62.01	75.79	54.61	66.38
Mean	28.56	36.54	47.81	73.61	49.57	55.54
Std. Error of Mean	6.108	7.283	6.335	1.538	3.28	3.632
p-value			0.0002 ***			

****significant p-value ≤0.0001*

3.13. Investigation of effect of Oxazine Derivative (A9) on growth cells (HRT) cells

The effect of Derivative (A9) on the growth process of colon cancer cell lines was studied, as it gave high percentage of inhibition to the growth of colon cancer cell lines at all concentrations which ranges 81.29% at 250 (µg/ml) to 87.1% at 1000 (µg/ml). As shown in **Figure 20** and **Table 3**, the concentration of the half-inhibitor (IC_{50}) was 0.1669 (µg/ml) [38, 39].

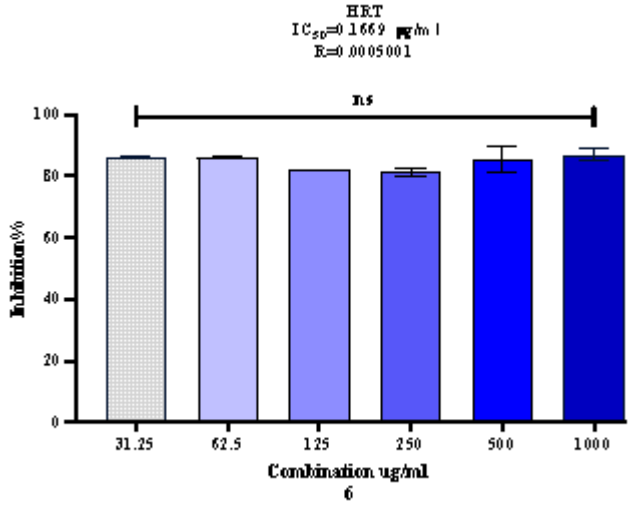

Figure 20. Comparison of mean values of Derivative (A9) in different concentrations. The figure shows a no significant difference among concentrations (p-value = 0.2426). Data are expressed as means ± SEM

Table 3. Comparison of mean values of Derivative (A9) in different concentrations

Concentration µg/ml	31.25	62.5	125	250	500	1000
Number of values	4	4	4	4	4	4
Minimum	85.28	85.66	81.82	78.36	77.59	82.59
Maximum	86.94	86.68	82.33	83.48	96.54	92.45
Mean	86.11	86.24	81.98	81.29	85.5	87.1
Std. Error of Mean	0.364	0.2367	0.1212	1.095	4.3	2.027
p-value			0.2426 ns			

ns: no significant p-value >0.05

4. Conclusion

In conclusion, the current work successfully demonstrated the synthesis of a series of heterocyclic derivatives based on trimethoprim, including azo, chalcone, pyrazoline, thiazine, and oxazine structures. These compounds were synthesized through efficient chemical transformations and confirmed by spectroscopic techniques. The observed physical properties underscored their structural variation and stability. Biological assessments against HRT colon cancer cells revealed promising cytotoxic effects, particularly for thiazine derivative (A8) and oxazine derivative (A9). Notably, A9 exhibited exceptional inhibitory activity with a very low IC_{50} value, suggesting its potential as a potent anticancer compound. These findings emphasize the value of trimethoprim as a versatile starting material for the development of novel therapeutic agents. The study offers a meaningful advancement in heterocyclic drug design and provides a foundation for future research into the biological evaluation and mechanism of action of these compounds, supporting their further development as candidates in cancer chemotherapy.

Conflict of interest

The authors declare no conflict of interest.

References

1. Khdera HA. Design, synthesis and characterization of new azoflavone derivatives through diazotisation - coupling reactions of aromatic amines (sulfanilic acid, 2-amino pyridine). Current Chemistry Letters. 2024;13(3):477-82.

2. Ali MM, Mhaibes RM, Othman MAM, Lahhob QR, Qasim MJ. Association between triglyceride-glucose index and risk of chronic kidney disease: a systematic review and meta-analysis. Journal of Nephropharmacology. 2024;13(2).
3. AlSaadi EK, Darweesh MA, Al Jawadi HF, Othman MAM. Demographic Characteristics, Clinical Features, Laboratory, and Radiological Findings in Children Admitted to COVID19 Center in Amara City, Misan Province, Iraq. Journal of Medicinal and Chemical Sciences. 2023;6(1):34-43.
4. Gleckman R, Blagg N, Joubert DW. Trimethoprim: mechanisms of action, antimicrobial activity, bacterial resistance, pharmacokinetics, adverse reactions, and therapeutic indications. Pharmacotherapy: The Journal of Human Pharmacology and Drug Therapy. 1981;1(1):14-9.
5. Eliopoulos GM, Huovinen P. Resistance to trimethoprim-sulfamethoxazole. Clinical infectious diseases. 2001;32(11):1608-14.
6. Shaaban MR, Mayhoub AS, Farag AM. Recent advances in the therapeutic applications of pyrazolines. Expert opinion on therapeutic patents. 2012;22(3):253-91.
7. Hmood NA, Othman MAM, Ali MM. Transcription factor 7-like 2 gene polymorphisms rs7903146associationwith type 2 diabetic polycystic ovarian syndrome women of Iraqi Population. Annals of Tropical Medicine and Public Health. 2019;22(12).
8. Kumar S, Bawa S, Drabu S, Kumar R, Gupta H. Biological activities of pyrazoline derivatives-A recent development. Recent patents on anti-infective drug discovery. 2009;4(3):154-63.
9. Al-Suraify SMT. Synthesis and characterization of novel compounds derived from 6-methyl-2,6 dihydro[1,2,4-triazino[4,3-b] indazol-3(4h)-one. International Journal of Pharmaceutical Research. 2020;12:1504-17.
10. Al-Suraify SMT. Synthesis and characterization of new heterocyclic compounds in corporating heterocyclic moiety derived from 3-chloro-1-methyl-1h-indazole. Biochemical and Cellular Archives. 2020;20:4127-34.
11. Al-Suraify SMT, Mekky AH, Husssien LB. Synthesis of new nitrogenous derivatives based on 3-chloro–1-methyl-1H-indazole. International Journal of Pharmaceutical Research. 2020;12:793-802.
12. Gupta N, Saini V, Basavarajaiah S, Dar MO, Das R, Dahiya RS. 1, 3-Oxazine as a promising scaffold for the development of biologically active lead molecules. ChemistrySelect. 2023;8(39):e202301456.
13. Al-Suraify SMT, Hussien LB. Synthesis and characterization of new compounds derived from 1H-indol-5-ylamine. Applied Nanoscience (Switzerland). 2023;13(3):2083-92.
14. Mahdi MA, Jasim LS, Mohamed MH. Synthesis and anticancer activity evaluation of novel ligand 2- [2 - (5-Chloro carboxy phenyl) Azo] 1-Methyl Imidazole (1-Mecpai) with Some Metal Complexes. Systematic Reviews in Pharmacy. 2020;11(12):1979-87.
15. Alshamusi QKM, Alzayd AAM, Mahdi MA, Jasim LS, Aljeboree AM. ADSORPTION OF CRYSTAL VIOLATE (CV) DYE IN AQUEOUS SOLUTIONS BY USING P(PVP-CO-AAM)/GO COMPOSITE AS (ECO-HEALTHY ADSORBATE SURFACE): CHARACTERIZATION AND THERMODYNAMICS STUDIES. Biochemical and Cellular Archives. 2021;21:2423-31.
16. Abdulsahib WK, Sahib HH, Mahdi MA, Jasim LS. Adsorption Study of Cephalexin Monohydrate Drug in Solution on Poly (vinyl pyrrolidone-acryl amide) Hydrogel Surface. International Journal of Drug Delivery Technology. 2021;11(4):1169-72.
17. Aljuaid A, Allahyani M, Alsaiari AA, Almehmadi M, Alsharif A, Asif M. Green Synthetic Methods of Oxazine and Thiazine Scaffolds as Promising Medicinal Compounds: A Mini-review. Current Organic Synthesis. 2024;21(7):837-57.
18. Salih TM, Jawad AA, Gouda MA, Abbas AK, Al-Tabra RH. Thiazine: Synthesis and Biological Activity. Magazine of Al-Kufa University for Biology. 2024;16(3).
19. Kianipour S, Razavi FS, Hajizadeh-Oghaz M, Abdulsahib WK, Mahdi MA, Jasim LS, Salavati-Niasari M. The synthesis of the P/N-type NdCoO3/g-C3N4 nano-heterojunction as a high-performance photocatalyst for the enhanced photocatalytic degradation of pollutants under visible-light irradiation. Arabian Journal of Chemistry. 2022;15(6).
20. Mahdi MA, Oroumi G, Samimi F, Dawi EA, Abed MJ, Alzaidy AH, Jasim LS, Salavati-Niasari M. Tailoring the innovative Lu2CrMnO6 double perovskite nanostructure as an efficient electrode materials for electrochemical hydrogen storage application. Journal of Energy Storage. 2024;88.
21. Radhy ND, Jasim LS. A novel economical friendly treatment approach: Composite hydrogels. Caspian Journal of Environmental Sciences. 2021;19(5):841-52.
22. Karim AN, Jasim LS. Synthesis and characterization of poly (CH/AA-co-AM) composite: Adsorption and thermodynamic studies of benzocaine on from aqueous solutions. International Journal of Drug Delivery Technology. 2019;9(4):558-62.
23. Choudhary S, Silakari O, Singh PK. Key updates on the chemistry and biological roles of thiazine scaffold: a review. Mini Reviews in Medicinal Chemistry. 2018;18(17):1452-78.
24. Patel G, Shah VR, Nguyen TA, Deshmukh K. Spirooxindole: Chemistry, synthesis, characterization and biological significance: Elsevier; 2024.
25. Drakontaeidi A, Papanotas I, Pontiki E. Multitarget pharmacology of sulfur–nitrogen heterocycles: anticancer and antioxidant perspectives. Antioxidants. 2024;13(8):898.

26. Batool M, Haider MN, Javed T. Applications of spectroscopic techniques for characterization of polymer nanocomposite: A review. Journal of Inorganic and Organometallic Polymers and Materials. 2022;32(12):4478-503.
27. Jamel HO, Jasim MH, Mahdi MA, Ganduh SH, Batool M, Jasim LS, Haider MN. Adsorption of Rhodamine B dye from solution using 3-((1-(4-((1H-benzo[d]imidazol-2-yl)amino)phenyl)ethylidene)amino)phenol (BIAPEHB)/P(AA-co-AM) composite. Desalination and Water Treatment. 2025;321.
28. Majeed HJ, Idrees TJ, Mahdi MA, Abed MJ, Batool M, Yousefi SR, Thumma A, Jasim LS. Synthesis and application of novel sodium carboxy methyl cellulose-g-poly acrylic acid carbon dots hydrogel nanocomposite (NaCMC-g-PAAc/CDs) for adsorptive removal of malachite green dye. Desalination and Water Treatment. 2024;320:100822.
29. Javed T, Kausar F, Zawar MD, Khalid N, Thumma A, Ismail A, Alzaidy AH, Abed MJ, Jasim LS, Taj MB, Tirth V, Haider MN. Investigating the adsorption potential of coconut coir as an economical adsorbent for decontamination of lanthanum ion from aqueous solution. Journal of Dispersion Science and Technology. 2024.
30. Shah A, Arjunan A, Manning G, Batool M, Zakharova J, Hawkins AJ, Ajani F, Androulaki I, Thumma A. Sequential novel use of Moringa oleifera Lam., biochar, and sand to remove turbidity, E. coli, and heavy metals from drinking water. Cleaner Water. 2024;2:100050.
31. Aljamali NM, Farhan ZM. Anticancer study of innovative macrocyclic formazan compounds from trimethoprim drug. Egyptian Journal of Chemistry. 2023;66(1):217-30.
32. Aljamali NM, Alsabri IKA. Development of trimethoprim drug and innovation of sulfazane-trimethoprim derivatives as anticancer agents. Biomedical and Pharmacology Journal. 2020;13(2):613-25.
33. Abbas AM, Nasrallah HH, Aboelmagd A, Boyd WC, Kalil H, Orabi AS. Novel Trimethoprim-Based Metal Complexes and Nanoparticle Functionalization: Synthesis, Structural Analysis, and Anticancer Properties. Inorganics. 2025;13(5):144.
34. Mohammed abd al-khaliq Z. Synthesis, characterization and antibacterial activity of new series of sulfamethoxazole derivatives". Ministry of Higher Education. 2015.
35. Ware D. Synthesis and Biological Evaluation of Nitrogen and Sulphur Containing Heterocyclic Compounds: Institute of Science, Nirma University; 2021.
36. Eugene-Osoikhia TT, Olawoyin AS, Aasegh TJ, Odozi NW, Ojo ND, Oyetunde T, Yeye EO, Akong RA, Onche EU, Oyeneyin OE. Facile synthesis, characterization, molecular and dynamic optical properties of metronidazole and sulfamethoxazole adducts of tricarbonyl (1-5-η-2-methoxycyclohexadienylium) iron. Discover Chemistry. 2025;2(1):1-21.
37. Bilyi AK, Antypenko LM, Ivchuk VV, Kamyshnyi OM, Polishchuk NM, Kovalenko SI. 2-Heteroaryl-[1, 2, 4] triazolo [1, 5-c] quinazoline-5 (6 H)-thiones and Their S-Substituted Derivatives: Synthesis, Spectroscopic Data, and Biological Activity. ChemPlusChem. 2015;80(6):980-9.
38. Mohamed H, Al-Ghareeb M, Abd-Allah R. Pharmacological evaluation of novel 1, 2, 4-triazine derivatives containing thiazole ring against hepatocellular carcinoma. Current Bioactive Compounds. 2022;18(2):12-25.
39. Reddy GS, Rao AV, Prasad MSN, Viswanath IVK, Laxminarayana E. Some new 1, 2, 4-triazole derivatives bearing the pyrimidine moiety as potential antimycobacterial agents: Synthesis and docking analysis. Letters in Drug Design & Discovery. 2023;20(10):1664-74.
40. Shakerimoghaddam A, Majeed HJ, Hashim AJ, Abed MJ, Jasim LS, Salavati-Niasari M. Green synthesis and characterization of NiO/Hydroxyapatite nanocomposites in the presence of peppermint extract and investigation of their antibacterial activities against Pseudomonas aeruginosa and Staphylococcus aureus. Results in Chemistry. 2025;13.